Making a Cool Choice: The Materials Library of Magnetic Refrigeration

Gottschall, Tino; Skokov, Konstantin P.; Fries, Maximilian et al.

(2019)

ADVANCED ENERGY MATERIALS
www.advenergymat.de

Making a Cool Choice: The Materials Library of Magnetic Refrigeration

Tino Gottschall, Konstantin P. Skokov, Maximilian Fries, Andreas Taubel, Iliya Radulov, Franziska Scheibel, Dimitri Benke, Stefan Riegg, and Oliver Gutfleisch**

The phase-down scenario of conventional refrigerants used in gas–vapor compressors and the demand for environmentally friendly and efficient cooling make the search for alternative technologies more important than ever. Magnetic refrigeration utilizing the magnetocaloric effect of magnetic materials could be that alternative. However, there are still several challenges to be overcome before having devices that are competitive with those based on the conventional gas–vapor technology. In this paper a rigorous assessment of the most relevant examples of 14 different magnetocaloric material families is presented and those are compared in terms of their adiabatic temperature and isothermal entropy change under cycling in magnetic-field changes of 1 and 2 T, criticality aspects, and the amount of heat that they can transfer per cycle. The work is based on magnetic, direct thermometric, and calorimetric measurements made under similar conditions and in the same devices. Such a wide-ranging study has not been carried out before. This data sets the basis for more advanced modeling and machine learning approaches in the near future.

1. Introduction

Solid-state magnetic refrigeration near room temperature is a relatively new and expanding field of material science[1–5] and engineering.[6–8] Worldwide, there are many prototype devices utilizing the magnetocaloric effect in order to demonstrate a thermal span and a cooling power.[9,10] However, there is still no mass-market product available for sale.[8] This is because, prior to any commercialization of magnetic refrigeration, a number of challenges need to be met. The conventional gas-compression technology for domestic cooling has been available for about 100 years and approximately one billion such refrigerators are in use today.[11] In order to compete successfully with conventional refrigeration technology, magnetic refrigeration must be more energy efficient, less costly, environmentally friendly, comparable in weight and volume, and less noisy.

Figure 1 illustrates schematically the different requirements necessary to develop magnetic cooling, from the fundamental science to the application. First of all, the reversible adiabatic temperature change ΔT_{ad} should be as large as possible in small magnetic-field changes because the ΔT_{ad} is directly related to the temperature span of the working device.[12] Equally important is the reversible isothermal entropy change Δs_T, which defines how much heat can be transferred in one cooling cycle.[13] In addition to these primary magnetocaloric properties, there are also secondary quantities that have to be taken into consideration. The isothermal entropy and the adiabatic temperature change are related via the heat capacity c_p, since $\Delta T_{ad} \approx \frac{-T\Delta s_T}{c_p}$. This means that a material with a low heat capacity has the potential to result in larger temperature changes. The benchmark magnetocaloric material, gadolinium, has a rather low c_p and therefore a large temperature change is obtained even though Δs_T is only moderate. Instead of pure metals, alloys and intermetallic compounds consist of 2, 3, or even more atomic species, which means that there are more degrees of freedom in the phononic system and the heat capacity of the lattice is increased. This is one reason why it is difficult for the more complex materials to reach similar temperature changes like those observed for the pure element gadolinium.

Since the magnetic field source is the most expensive part of any magnetocaloric cooling device, the volume in which the magnetic field is applied should be used as efficiently as possible.[14] For this reason, the volumetric entropy change is more relevant for applications than the specific entropy change, with both parameters being linked by the density ρ. This is an issue, especially for alloys produced by a solid-state reaction that contain some residual porosity.[15]

For a magnetic refrigerator, an operating frequency of several Hz is desirable,[9] which results in certain requirements

Dr. T. Gottschall
Dresden High Magnetic Field Laboratory (HLD-EMFL)
Helmholtz-Zentrum Dresden-Rossendorf
01328 Dresden, Germany
E-mail: t.gottschall@hzdr.de

Dr. T. Gottschall, Dr. K. P. Skokov, Dr. M. Fries, A. Taubel, Dr. I. Radulov, Dr. F. Scheibel, D. Benke, Dr. S. Riegg, Prof. O. Gutfleisch
Technische Universität Darmstadt
Institut für Materialwissenschaft
Alarich-Weiss-Str. 16, 64287 Darmstadt, Germany
E-mail: gutfleisch@fm.tu-darmstadt.de

The ORCID identification number(s) for the author(s) of this article can be found under https://doi.org/10.1002/aenm.201901322.

DOI: 10.1002/aenm.201901322

regarding the chosen magnetocaloric material. First of all, the transformations taking place in the magnetocaloric material have to be fast enough to follow the magnetic field, which turns out not to be a problem for most compounds.[16,17] Much more of a problem is the heat exchange between the magnetocaloric material and the fluid, which means the thermal conductivity λ of the material should be maximized.[18] However, the surface area and its characteristics are also important. Most simple heat exchangers are made of loose powder, providing good filling factors and a simple transfer of heat to the fluid.[19] On the other hand, with decreasing powder size the pressure drop and therefore the losses increase.[20] Another promising approach to provide a good heat exchange without large pressure drops is the use of plates or fine-structured magnetocaloric materials with an extended surface area.[21] However, this requires that the magnetocaloric material is machinable into the desired shape without any reduction in performance.[22] The rapidly developing field of additive manufacturing could be the route to producing complex heat-exchanger structures with an efficient exchange of heat.[23,24]

Finally, the magnetocaloric alloy should contain no harmful or critical elements, in order to possess a low environmental footprint.[12] At the same time, the material must be capable of operating for millions of cycles without any fatigue.[25] And since the refrigerant is in permanent contact with the heat-exchange fluid, long-term corrosion resistance must be guaranteed too.[26]

All these different aspects determine the thermal span, the cooling power and, therefore, the efficiency of the magnetic cooling device. But in fact, there is a huge gap between the fundamental material science and the realizable applications. For instance, the thermodynamic conditions in a magnetocaloric refrigerator are never ideally adiabatic or isothermal, but something in between. Moreover, the standard characterization of ΔT_{ad} and Δs_T typically involves bulk samples.[16,27,28] On the other hand, a magnetocaloric heat exchanger requires materials in the form of loose powder or fine structures in the submillimeter range.[10,29,30] However, it has been shown in the literature that the magnetocaloric properties on these different length scales do not necessarily coincide.[31,32] In the case of hysteretic materials, it also needs to be remembered that often the magnetocaloric properties are only provided for the first field application and are not always relevant for cycling.[33]

In this study we want to provide a profound material analysis to make the selection of materials easier and make it possible to assess the suitability of magnetocaloric materials for a particular application. First, we briefly introduce the different facets of the magnetocaloric effect by means of three important materials. Subsequently, we compare a large number of compounds with the benchmark material, gadolinium, in terms of their reversible magnetocaloric performance, criticality aspects, and the amount of heat that can be transferred in each cycle. All this has often been overlooked in literature.

Tino Gottschall is a postdoctoral researcher in the High Magnetic Field Laboratory at Helmholtz-Zentrum Dresden-Rossendorf, Germany. He studied physics at the Technical University Dresden, Germany, and finished his Diploma in 2012. He received his Ph.D. degree from the Technical University Darmstadt, Germany, in 2016. His research focuses on the magnetic and multicaloric properties of functional materials.

Konstantin P. Skokov is a senior researcher in the functional materials group at the Technical University Darmstadt, Germany. He received his Ph.D. in physics at the Tver State University, Russia in 1998. From 2008 to 2012 he was a scientist at Leibniz Institute IFW Dresden, Germany. His research interests are focused on the study of novel materials for magnetocaloric application and energy conversion as well as the development of unique scientific instrument for advanced characterization of magnetic materials.

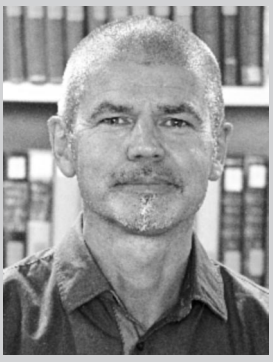

Oliver Gutfleisch is a full professor of functional materials at Technical University Darmstadt and a scientific manager at Fraunhofer IWKS Materials Recycling and Resource Strategies Hanau, Germany. His interests span from new permanent magnets for power applications to energy-efficient magnetic cooling, ferromagnetic shape-memory alloys, and magnetic nanoparticles for biomedical applications, with particular emphasis on tailoring structural and chemical properties on the nanoscale. Resource efficiency on element, process, and product levels, as well as recycling of strategic metals, are also in the focus of his work. He was awarded an ERC Advanced Grant on caloric cooling in 2017.

2. About the Manifestation of the Magnetocaloric Effect in Different Types of Materials

This section gives an overview of the two types of transitions we can encounter in magnetocaloric materials defined by the thermodynamic order of the transformation. We speak about a first-order transition when the order parameter, e.g., magnetization in the case of magnetocaloric materials, changes discontinuously with the temperature,[34] whereas a continuous

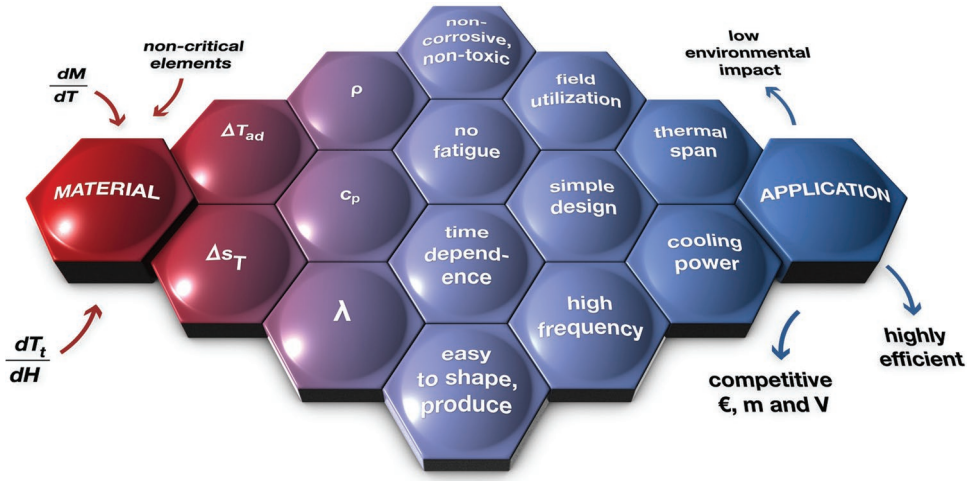

Figure 1. Illustration of the different challenges for magnetic refrigeration with respect to applications. This roadmap is directly transferable to the other caloric effects as well.

change implies a second-order transition.[35,36] The latter is, for instance, the case for a pure magnetic transition between a para- and ferromagnetic phase around the Curie temperature T_C. The perfect material example is the element gadolinium, with its T_C near room temperature. As shown in **Figure 2**a, the magnetization vanishes continuously at the Curie temperature, at least in low magnetic fields. The corresponding temperature dependence of the entropy s is plotted in Figure 2b. Applying a magnetic field introduces an additional ordering of the magnetic moments in the ferromagnetic phase against thermal fluctuations, but also a certain induced magnetization is observed in the paramagnetic phase as well, leading to a smoothing of the curve (see Figure 2a). Due to this increasing magnetic order, the entropy is lowered in magnetic fields, as can be seen in Figure 2b. Further details on the sample preparation and experimental techniques can be found in the Supporting Information.

The response of a material when it is being magnetized depends on the thermodynamic conditions under which the magnetic field is applied. At a constant temperature, a decrease in the entropy is observed and we speak about the isothermal entropy change Δs_T. Under these conditions, the state of the sample moves along a vertical path in the $s(T)$ diagram, indicated by a vertical arrow in Figure 2b. However, under adiabatic conditions the entropy is kept constant and therefore the system follows a horizontal path by increasing the sample's temperature (horizontal arrow in Figure 2b). The corresponding adiabatic temperature ΔT_{ad} and isothermal entropy change Δs_T values are plotted as a function of the starting temperature for magnetic field changes of 1 and 2 T in Figure 2c. In applied field below 10 T, the maximum magnetocaloric effect is always observed at the Curie temperature. However, in high fields it has been shown that the position of the maximum is shifting toward higher temperatures.[37]

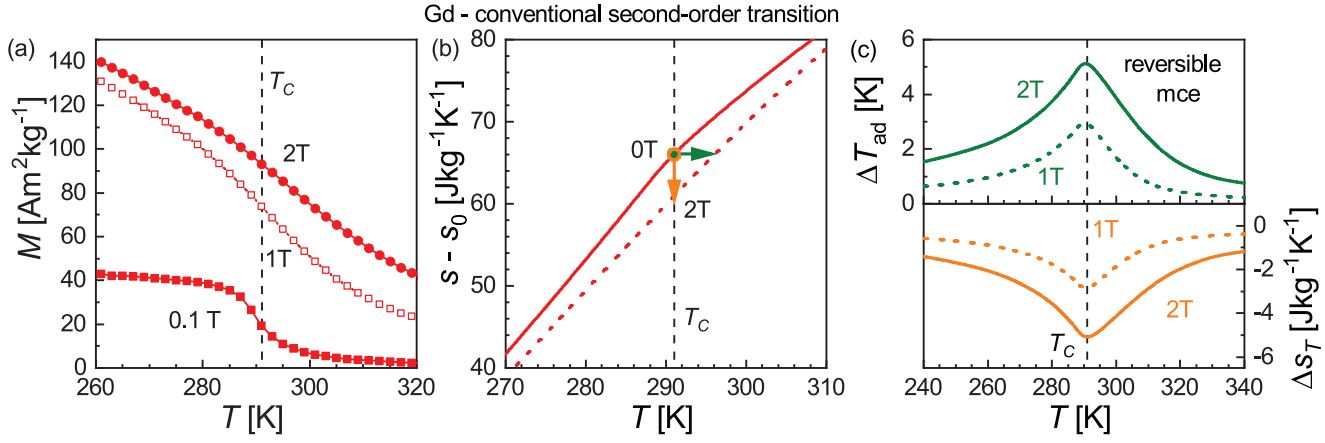

Figure 2. Magnetic and magnetocaloric properties of gadolinium. a) Magnetization measurements in 0.1, 1, and 2 T. In low fields the magnetization vanishes at the Curie temperature T_C. b) Total entropy related to a reference entropy s_0 as a function of temperature in 0 and 2 T. The vertical arrow indicates the respective Δs_T and the horizontal arrow, the ΔT_{ad} when applying a magnetic field of 2 T. c) The corresponding values of the magnetocaloric effect are plotted as a function of temperature.

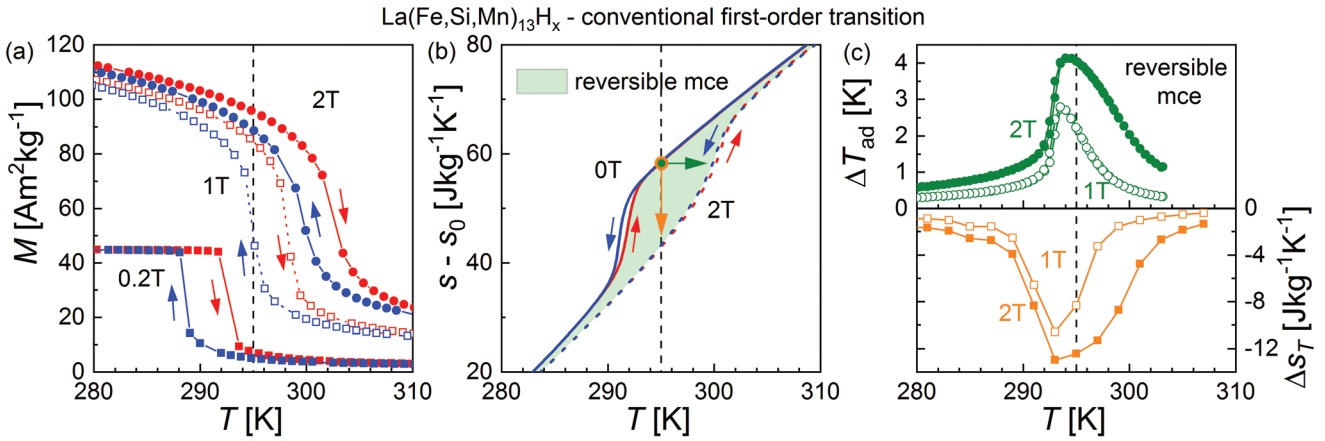

Figure 3. Magnetic and magnetocaloric properties of La(Fe,Si,Mn)$_{13}$Hx. a) Magnetization measurements in 0.2, 1, and 2 T. At the transition temperature T_t, the magnetization drops. b) Total entropy related to a reference entropy s_0 as a function of temperature under heating and cooling in 0 and 2 T. The vertical arrow indicates the respective Δs_T and the horizontal arrow, the ΔT_{ad} when applying a magnetic field of 2 T. c) The corresponding values of the magnetocaloric effect are plotted as a function of temperature.

Materials with a first-order transition have, by definition, a discontinuity in their entropy. A further classification can be undertaken by considering how the material reacts on magnetic field application. Historically, the warming of a material in a magnetic field is declared to be the conventional magnetocaloric effect (MCE). On the other hand, a decrease in temperature is observed when a so-called inverse magnetocaloric material is magnetized.[38] It is worth noting that despite the different facets, the physics behind is the same.

An important example of such a transformation for the conventional type are the 1:13-based alloys La(Fe,Si)$_{13}$.[13] **Figure 3** shows the case for La(Fe,Si,Mn)$_{13}$Hx. The binary material Fe$_{0.51}$Rh$_{0.49}$ undergoes a transition with an inverse effect[39,40] instead, which is summarized in **Figure 4** (see the Supporting Information for further information). Such a first-order transition is denoted either as a magnetostructural or magnetoelastic transformation. In the first case, the magnetization change is linked to a structural conversion between two phases with different magnetizations[41] whereas a change in the lattice parameters is caused in the magnetoelastic case.[42] As a consequence, typically, an abrupt change in magnetization is observed, as clearly shown in the Figures 3a and 4a. However, it is worth noting that the characteristics of materials in real experiments are not generally as distinct as in the ideal case.

The application of a magnetic field has a quite different effect on a first-order magnetostructural transition in comparison to the purely magnetic second-order type. It is found that the transition temperature shifts to higher (conventional) or lower (inverse) temperatures, since the magnetic field stabilizes the phase with the higher magnetization. For this reason, a conventional first-order material like La–Fe–Si increases its transition temperature under the influence of a magnetic field, whereas a lowering of the transition temperature is observed in an inverse magnetocaloric material like Fe–Rh. The corresponding entropy–temperature diagrams are plotted for heating and cooling in magnetic fields of 0 and 2 T as solid and dashed

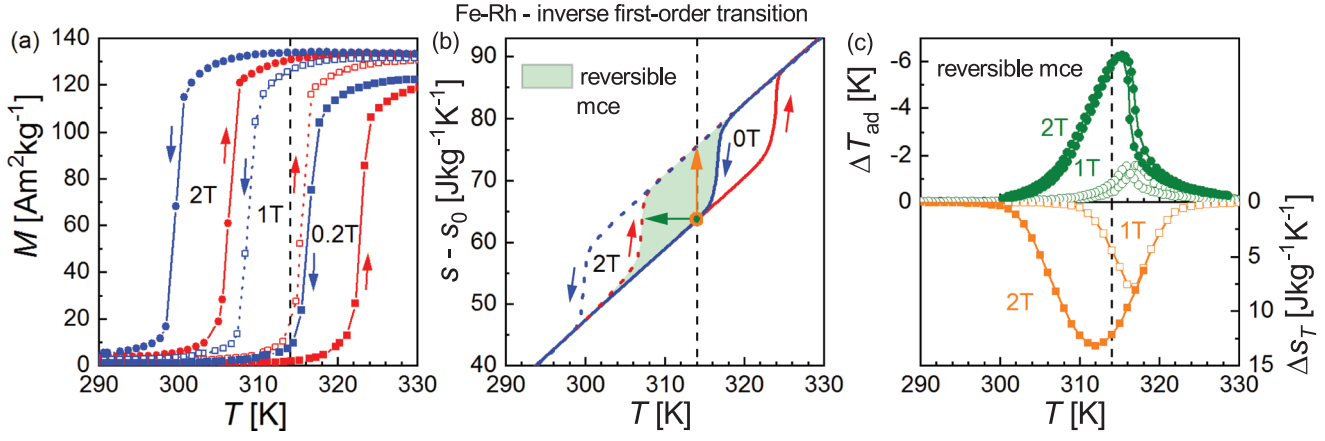

Figure 4. Magnetic and magnetocaloric properties of Fe–Rh. a) Magnetization measurements in 0.2, 1, and 2 T. At the transition temperature T_t, the magnetization increases jump-like. b) Total entropy related to a reference entropy s_0 as a function of temperature under heating and cooling in 0 and 2 T. The vertical arrow indicates the respective Δs_T and the horizontal arrow, the ΔT_{ad} when applying a magnetic field of 2 T. c) The corresponding values of the magnetocaloric effect are plotted as a function of temperature.

lines in Figures 3b and 4b, respectively. The shift of the transition temperature is also apparent in those plots, whereby the $s(T)$ diagram takes the shape of a parallelogram.

In fact, the manifestation of the structural change—being the underlying cause of the magnetocaloric effect—can be very different, depending on the material. Compounds like Heusler alloys typically transform between a cubic austenite and a tetragonal or orthorhombic martensite phase, with a discrete volume and aspect-ratio change of the unit cell.[43] Other materials, like the presented La–Fe–Si system, transform between two cubic phases, having a significantly different unit-cell volume, accounting for about 1%.[44] We could also speak of an isostructural phase transition in this case as well. The same applies basically to Fe_2P-type compounds, transforming from one hexagonal phase to another.[45] In this particular material family, the lattice parameters change in opposite directions, with the consequence that there might be no overall volume change, even though the lattice mismatch is substantial.

All these first-order materials have in common that they transform in avalanches via a nucleation-and-growth process. This discontinuous type of transition always causes a certain hysteresis, and for this reason the heating and cooling curves of the total entropy and the magnetization in Figures 3 and 4 do not coincide. The occurrence of thermal hysteresis has dramatic consequences for the magnetocaloric properties, because the magnetostructural transition is not completely reversed after the application of a magnetic field, which decreases the reversible magnetocaloric effect. A fully reversible transformation and magnetocaloric effect can only be observed within the highlighted area. The plots in Figures 3c and 4c illustrate the reversible adiabatic temperature change ΔT_{ad} and the isothermal entropy changes Δs_T under cycling in magnetic fields of 1 and 2 T. The corresponding paths during the thermodynamic processes are illustrated in the $s(T)$ diagrams as horizontal and vertical arrows, as for gadolinium in Figure 2.

The shapes of the ΔT_{ad} and Δs_T curves of the two first-order materials shown in Figures 3c and 4c are fundamentally different to the behavior observed for gadolinium in Figure 2c. The magnetocaloric effect of the second-order material Gd always reaches its maximum at the Curie temperature T_C, independent of the field strength, since the derivative $\left(\frac{\partial M}{\partial T}\right)_H$ is the largest at this point. For a first-order transition, the position of the maxima in ΔT_{ad} and Δs_T are changing with an increasing magnetic field. However for a first-order transition with a conventional magnetocaloric effect, the decay of the left flank of the peak always follows the same trend (right flank for the inverse magnetocaloric effect), because at low temperatures the ferromagnetic phase is already present and an increase in the magnetic field cannot induce any further transformation.

When the magnetic field is large enough, the transition might be completed and a plateau-like behavior of the magnetocaloric effect is observed. The width of this plateau is determined by the shift of the transition temperature in magnetic field and therefore it broadens when higher field are applied.[46] However, in fields up to 2 T, the operational window of first-order materials is rather narrow in comparison to systems with a purely magnetic transition. For this reason, stacked heat exchangers with many different T_t are required in order to provide a sufficiently wide temperature window for the machine.[47]

3. Comparison of the Reversible Magnetocaloric Properties

In the following, a profound comparison of different magnetocaloric materials will be made, considering the temperature and entropy changes under cyclic conditions. In particular for hysteretic materials, special care is required in order to determine the magnetocaloric properties under cycling in a reasonable manner.[39,48,49] The measurement setups and protocols are described in detail in the Supporting Information.

The Ashby-like plots in **Figure 5**a,b combine real measurements of the reversible magnetocaloric effect of a large number of materials—each circle stands for a single sample. The reversible adiabatic temperature change ΔT_{ad} as a function of the individual transition temperatures T_t in 2 T in (a) and 1 T in (b) is represented by the y axis. The third dimension, i.e., the area of the scatters, indicates the corresponding isothermal entropy change Δs_T under cycling in the same magnetic field change, whereas the scale is shown on the right of Figure 5. Dashed curves are introduced as a guide to the eye, connecting the different data points of the same material family, providing a pathway for the tunability range of the system.

From the scatter diagram it is apparent how strongly the magnetocaloric effect is dependent on the transition temperature. For instance, in the system $La(Fe,Si,Co)_{13}$, ΔT_{ad} and Δs_T are more than halved when the transition is shifted from below 200 K to room temperature by a compositional variation.[50] This is a critical issue for a magnetic refrigerator with stacks of different materials to facilitate wide temperature spans. Thus, for future applications it is probably more favorable to combine different material families working at selected temperature ranges, and giving their best performance, rather than focusing on a single material family. A comprehensive table of all the important properties of the magnetocaloric materials can be found in **Table 1**.

Around room temperature, there are several material families showing reasonable magnetocaloric effects in 2 T. For instance, Mn–Fe–P–Si and $La(Fe,Mn,Si)_{13}H_y$ can compete with Gd in terms of ΔT_{ad}, but their corresponding Δs_T is several times larger due to the first-order nature of the transition. This means that these compounds are capable of pumping much more heat in a single cooling cycle. Even larger reversible adiabatic temperature changes than in Gd can be obtained using FeRh or Gd–Si–Ge. One reason for this is that both materials show a strong first-order character and therefore the shift of the transition temperature—the driving force of the magnetocaloric effect—is large. However, this comes at the price of a rather large thermal hysteresis. The consequences of this are impressively shown in Figure 5b for a cyclic magnetic field of only 1 T. Here, both materials fall behind most other compounds and have little more than 1.2 K of reversible temperature change. The influence of the thermal hysteresis on the magnetocaloric properties under cycling becomes even more apparent for the example of Ni–Mn–In–(Co) Heusler alloys. While a modest reversible ΔT_{ad} is possible in a magnetic field change of 2 T, the cyclability disappears almost completely if only 1 T is available.

From our study it is clear that near room temperature and in a magnetic field change of 1 T, gadolinium is the best material in terms of the reversible ΔT_{ad}. The family $La(Fe,Mn,Si)_{13}H_y$

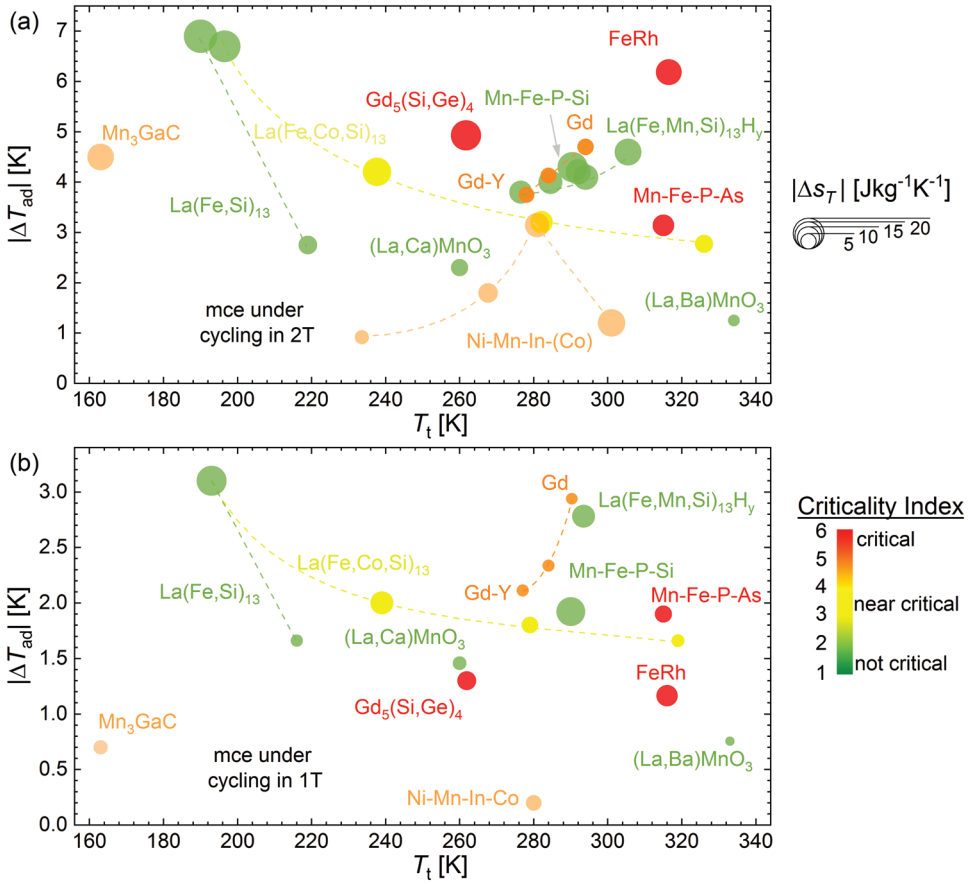

Figure 5. Ashby-like diagrams of magnetocaloric materials. These plots show both the reversible adiabatic temperature change ΔT_{ad} (y axis of the diagram) and the isothermal entropy change Δs_T (illustrated by the area of the spots) in a magnetic field change of a) 2 T and b) 1 T versus the operating temperature T_t. The criticality of the respective compounds is represented by the color of the data points. Every data point stands for a single sample.

comes second, with a smaller reversible magnetocaloric effect compared to Gd, but still the entropy change is several times larger.

4. Criticality of Materials

Gadolinium and Gd-based systems are widely used in demonstrators.[10,51] Even though the demand for gadolinium metal is at the moment lower than its current availability, this situation will reverse as soon as the need for this element increases, since the raw material deposits are limited.[52] Despite its outstanding magnetocaloric properties, Gd is not an option for the widespread use of magnetic refrigeration, since it is simply too critical and expensive.

For this reason we also want to consider sustainability aspects in order to allow a reasonable assessment of the suitability of potential systems. Therefore, the spots in Figure 5 are colored like a traffic-light scheme, from green for not critical to red for critical materials. The criticality assessment of the compounds shown in Figure 5 is based on a model taking into account the geological availability, geopolitical situation, recyclability, and sustainability.[53] The elements we consider in terms of their criticality are: As, Co, Fe, Gd, Ge, In, La, Mn, Ni, P, Rh, Si, according to the list of critical materials named by the European Commission.[54]

Whereas the elements Mn, Ni and Si hold no risk, Co, Ge, In, P, and Rh are highly critical because of their high supply risk and technological importance.[55] The light rare earths such as La are considered as by-products when mining for heavy-rare-earth elements and are therefore less problematic.[56] Instead, the large-scale use of the heavy rare earth Gd in magnetocaloric cooling devices is not favorable. Calculations show that the demand for this element would be higher than the current and future supply.[57] Hence, the use of compounds from the classes FeRh and $Gd_5(Si,Ge)_4$ are considered to be highly critical, since they contain large amounts of the elements Rh, Gd, and Ge. The medium-high risk of Ni–Mn–In–(Co) Heusler alloys is due to the requirements for In and Co. The complete or at least partial substitution of those critical elements is, as a result, an important goal. The $La(Fe,Si,Co)_{13}$ family has a medium-low risk because of the use of small amounts of Co. However, $La(Fe,Si,X)_{13}H_x$ has a low risk given the fact that La is (together with Ce) the least critical light-rare-earth element and highly abundant. Fe_2P-type materials are considered as noncritical, yet the use of toxic arsenic is not favorable in applications. The criticality of P in these compounds was assessed in ref. [57] and due to the small amounts used for magnetocaloric

Table 1. Comparison of the magnetocaloric properties of the most relevant materials. The table provides information about the nature of the transformation, chemical composition, transition temperature, adiabatic temperature and isothermal entropy change under cycling in 2 and 1 T, magnetization change, hysteresis width, shift of the transition temperature, heat capacity near the transition, thermal conductivity, density, reversible heat, relative cooling power (RCP), temperature averaged entropy change (TEC), criticality index (from 1 for not critical to 6 for highly critical) and the references.[13,40,48,60,64–70]

	Material	T_t [K]	ΔT_{ad} [K]	Δs_T [J kg^{-1} K^{-1}]	ΔT_{ad} [K]	Δs_T [J kg^{-1} K^{-1}]	ΔM [A m^2 kg^{-1}]	ΔT_{Hys} [K]	$\mu_0^{-1}dT_t/dH$ [K T^{-1}]	c_p (near T_t) [J kg^{-1} K^{-1}]	λ [W m^{-1} K^{-1}]	ρ [g cm^{-3}]	Q_{rev} [J g^{-1}]		RCP [J kg^{-1}]	TEC(3) [J K^{-1} kg^{-1}]	Criticality index	Ref.
			Under cycling in 2T		Under cycling in 1T								2 K, 2 T	3 K, 2 T	2 T	3 K, 2 T		
Conventional 2nd order	Gd	292.0	4.7	5.2	2.9	2.8	–	–	–	240	7.5	7.9	0.90	0.61	226.9	7.06	5	[a]
	$Gd_{98.7}Y_{1.3}$	284.0	4.1	5.0	2.3	3.0	–	–	–	n/a	n/a	7.9	n/a	n/a	214.5	4.99	5	[a]
	$Gd_{96.6}Y_{3.4}$	278.0	3.8	5.0	2.1	3.1	–	–	–	n/a	n/a	7.9	n/a	n/a	206.1	4.90	5	[a]
	$La_{0.7}Ca_{0.3}MnO_3$	260.0	2.3	5.7	1.5	3.6	–	–	–	530	1.5	5.8	0.40	0.00	98.5	5.40	1	[64][a]
	$La_{0.7}Ba_{0.3}MnO_3$	334.0	1.3	2.8	0.8	1.8	–	–	–	n/a	n/a	n/a	n/a	n/a	78.6	2.74	1	[64][a]
Conventional 1st order	$Gd_5Si_2Ge_2$	261.7	4.9	18.4	1.3	7.1	100	5.0	+4.9	330	n/a	6.7	n/a	n/a	195.3	18.20	6	[65][a]
	$LaFe_{11.6}Si_{1.4}$	190.0	6.9	21.7	3.1	17.4	85	1.5	+4.4	450	n/a	n/a	3.18	2.63	181.5	21.52	1	[66][a]
	$LaFe_{11.2}Si_{1.8}$	216.3	2.7	6.8	1.7	3.0	–	–	–	440	n/a	n/a	n/a	n/a	121.8	6.73	1	[a]
	$LaFe_{10.71}Co_{1.30}Si_{1.00}$	326.0	2.8	6.9	1.7	3.5	80	<1	+1.6	n/a	n/a	7.2	n/a	n/a	185.4	6.84	3	[13]
	$LaFe_{11.05}Co_{0.91}Si_{1.04}$	282.1	3.2	10.5	1.8	5.4	85	<1	+3.1	500	12.5	7.2	0.94	0.20	168.7	10.55	3	[13]
	$LaFe_{11.40}Co_{0.52}Si_{1.09}$	237.7	4.2	16.8	2.0	10.5	90	<1	+4.2	n/a	13.5	7.2	n/a	n/a	147.4	16.49	3	[13]
	$LaFe_{11.74}Co_{0.13}Si_{1.13}$	196.5	6.7	20.3	n/a	n/a	110	<1	+4.4	434	n/a	7.2	3.99	2.43	195.3	20.33	3	[13]
	$LaFe_{11.84}Mn_{0.34}Si_{1.30}H_x$	291.9	4.2	13.0	2.8	10.6	60	<1	+4.4	470	7.2	7.1	3.31	2.59	129.4	12.59	1	[67][a]
	$LaFe_{11.83}Mn_{0.32}Si_{1.30}H_x$	297.0	4.9	12.6	2.5	11.1	60	1.3	+4.6	475	n/a	7.1	2.38	1.70	105.6	12.24	1	[a]
	$MnFeP_{0.55}As_{0.45}$	315.0	3.1	9.2	1.9	5.8	80	5.0	+5.2	515	n/a	n/a	1.48	0.72	88.1	9.10	6	[60][a]
	$MnFe_{0.95}P_{0.585}Si_{0.34}B_{0.075}$	290.5	4.3	17.6	1.9	16.3	80	1.5	+4.0	625	n/a	5.7	3.15	1.97	128.2	16.97	1	[68][a]
Inverse 1st order	$Fe_{49}Rh_{51}$	316.5	6.2	13.2	1.2	9.4	130	7.1	–9.0	350	n/a	10.0	3.04	2.67	153.4	12.88	6	[40][a]
	$Ni_{50.2}Mn_{35.0}In_{14.8}$	301.0	1.2	15.0	0.0	0.0	58	3.6	–1.6	425	n/a	7.9	0.00	0.00	23.7	8.23	4	[48]
	$Ni_{49.6}Mn_{35.6}In_{14.8}$	267.7	1.6	7.5	0.0	0.0	80	7.9	–3.7	542	19.0	7.9	0.00	0.00	30.5	6.58	4	[48]
	$Ni_{49.8}Mn_{35.0}In_{15.2}$	233.6	0.9	4.0	0.0	0.0	80	14.4	–6.9	542	n/a	7.9	0.00	0.00	8.5	2.82	4	[48]
	$Ni_{45.7}Mn_{36.6}In_{13.5}Co_{4.2}$	288.9	3.0	10.5	0.2	5.0	110	10.0	–8.0	472	23.5	7.9	1.43	0.20	51.0	9.58	5	[69][a]
	Mn_3GaC	163.0	4.5	14.0	0.7	6.4	65	3.0	–6.0	412	n/a	6.9	n/a	n/a	112.7	12.65	4	[70][a]

[a] This work.

compounds in relation to the use of P in fertilizer, the future demand for solid-state refrigeration is assessed as noncritical.

5. The Reversible Heat as a Figure of Merit

For an honest assessment of the suitability of magnetocaloric materials, a reliable performance parameter—a figure of merit—is required. One attempt was made in terms of the relative cooling power RCP.[58,59] Quite contradictory details about its determination can be found in the literature.[18] Often, RCP is calculated by multiplying the width of the isothermal entropy change peak by its FWHM.[60] This kind of estimation raises up materials with a flat and broad Δs_T curve; however, it ignores many aspects, for instance, that most importantly both the ΔT_{ad} and Δs_T must be as large as possible in rather low cyclic magnetic-field changes.[61] Consequently, the relative cooling power is not sufficient, in order to compare the quality of magnetocaloric materials and to optimize them.[13]

The evaluation of the COP—the coefficient of performance—goes in a different direction. The aim is to estimate the ratio between the actual cooling power and the work that is required for a given thermodynamic cycle $\mathrm{COP} = \frac{P}{W}$.[51] The cooling power consists of the cooling power provided by the material minus the losses of the machine $P = P_{mat} - P_{loss}$. The losses, however, are specific for every machine and depend on the operating conditions. Since P_{loss} is unknown in most cases, the material COP was introduced, which is given by $\mathrm{COP}_{mat} = \frac{P_{mat}}{W}$ ignoring the losses.[62] This can lead to meaningless results, especially when the work goes to zero faster than the cooling power. When taking this parameter for optimization, it carries the risk of highlighting materials that are indeed efficient, but that can pump only very little heat.

Recently, Griffith et al. suggested the temperature-averaged entropy change TEC as a figure of merit.[63] It considers the average value of Δs_T for a certain temperature span. From Table 1 it is clear that TEC, for instance, for a span of 3 K and a field change of 2 T provides a much more realistic picture than RCP. The latter highlights materials with a broad transition, leading to arbitrary values in the sample series of La–Fe–Si–Co, whereas TEC(3) shows a monotonic decrease, in agreement with the trends for ΔT_{ad} and Δs_T. However, caution is advised when calculating TEC for unrealistically high temperature spans that are not obtainable with a single material. Instead, multiple stages with different transition temperatures would be required, which is much more complex to assess.

In this paper we prefer to focus on the transferable heat Q_{rev}, which can in principle be utilized in the cyclic operation of a machine for a given temperature span. From this parameter it is not possible to predict how efficient a magnetocaloric material would be in a magnetic cooling device, since this task can only be fulfilled on the basis of advanced modeling or even better by using the material in a real machine. However, estimating Q_{rev} for defined working conditions makes a reasonable assessment of the principle applicability of the material under consideration possible. We should state that this kind of analysis is not a new one; it is a fundamental aspect of thermodynamic cycles and has been discussed in the literature many times.[13,51,71]

Figure 6a,b shows the $s(T)$ diagrams of La–Fe–Si–Mn–H and Fe–Rh, respectively. The entropy as a function of magnetic field and temperature (cooling and heating curves) can be obtained experimentally, for instance, by calorimetric methods (see the Supporting Information). The area between the heating curve in zero field and the cooling curve in a field is the reversible part of the $S(T)$ diagram of a material showing a conventional magnetocaloric effect (highlighted). The reversible region of inverse materials such as Fe–Rh is defined by the zero-field cooling and the in-field heating curve, respectively. For an arbitrary temperature span of 3 K, the corresponding Carnot cycles of La–Fe–Si–Mn–H and Fe–Rh for a hot heat-exchanger temperature of 297 and 314 K are plotted in Figure 6a,b as rectangles filled with a line pattern. These rectangles coincide with the work involved per cycle. The respective transferable heat Q_{rev} is illustrated by the long rectangle with cross hatching. Depending on the nature of the magnetocaloric transition, it can be calculated by

$$Q_{rev} = \left(s_h(T_{cool}, H_0) - s_c(T_{hot}, H_1)\right) \cdot T_{cool} \quad (1)$$

for conventional materials and by

$$Q_{rev} = \left(s_c(T_{cool}, H_1) - s_h(T_{hot}, H_0)\right) \cdot T_{cool} \quad (2)$$

for inverse magnetocaloric materials for a certain temperature span defined by T_{cool} and T_{hot} and magnetic field change $\Delta H = H_1 - H_0$. s_h and s_c are the total entropy measured under the heating and cooling protocol. We want to emphasize that for a real magnetocaloric machine, the Carnot cycle is not realistic. Other thermodynamic cycles like the Brayton or Ericsson cycles are much better descriptions of the actual processes. However, when comparing Q_{rev}, the differences are insignificant, being below 1 %. For the purpose of a figure of merit, the transferable heat of the Carnot cycle is a reasonable approximation, enabling its estimation in a rather simple and elegant way. In fact, only two points of the $s(T)$ are required, in contrast to the Brayton or Ericsson cycles, where the integration of the entropy curves is necessary. The reader is referred to the literature on this topic.[51]

For the two samples, Q_{rev} in a magnetic field change of 2 T is plotted for temperature spans from 2 to 5 K as a function of the hot heat-exchanger temperature T_{hot} in Figure 6c,d. Such a representation is quite illustrative, because it directly shows the working range of a single-stage magnetocaloric heat exchanger, as well as the heat that the material could pump per cycle from the cold to the hot side of the machine. For the Fe–Rh sample, Q_{rev} builds a plateau, which is due to the special shape of the $s(T)$ diagram. Consequently, the height and the width of the plateau increase for lower temperature spans. A negative Q_{rev} means that a Carnot cooling cycle under the given conditions is not possible. For instance, a temperature span of 7 K would exceed the maximum adiabatic temperature change ΔT_{ad} of this material in a field change of 2 T and as a result, Equation (2) would always be negative and therefore this process is not feasible.

Special care must be taken when the first-order magnetocaloric material has a rather large thermal hysteresis and/or the shift of the transition is not sufficient to transform back and forth completely.[72] In this case, a minor loop of the hysteresis

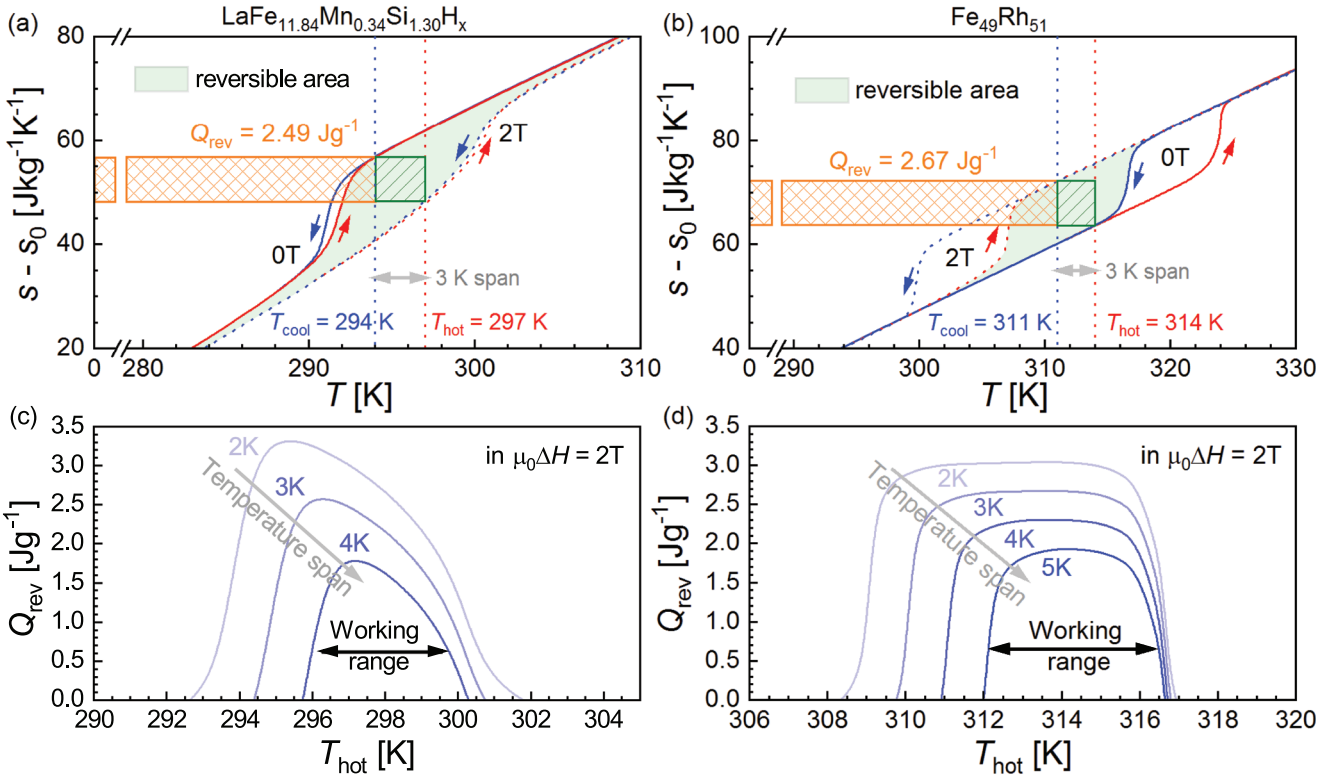

Figure 6. $s(T)$ diagram of a) the La–Fe–Si–Mn–H compound and b) Fe–Rh sample. The respective Carnot cycles for a hot and cold heat-exchanger temperature T_{hot} and T_{cool} are illustrated by the green rectangle. The resulting transferable heat Q_{rev} is shown as orange rectangles. c,d) Q_{rev} as a function of T_{hot} for different temperature spans. A negative value of Q_{rev} indicates that the corresponding Carnot cycle exceeds the potential of the magnetocaloric material.

is described and its reversibility area in the $s(T, H)$ diagram can deviate significantly from the scenario drawn above for La–Fe–Si and Fe–Rh. Consequently, the cyclic ΔT_{ad} and Δs_T cannot be predicted from basic thermodynamic considerations, based on isofield experiments alone. Instead, direct measurements under magnetic-field sweeping need to be performed.[72]

The calculated figure of merit Q_{rev} is plotted for different materials in **Figure 7** for Carnot cycles with temperature spans of 2 (solid curves) and 3 K (dashed curves) in a magnetic-field change of 2 T. This illustration allows us to compare and rate the usefulness of the available magnetocaloric materials. The temperature dependence of the specific Q_{rev} is shown in Figure 7a.

In a magnetocaloric refrigerator, the magnetized volume is the limiting factor and not the mass of the magnetocaloric material. For this reason, the volumetric Q_{rev} is plotted in Figure 7b too. In this picture, Fe–Rh is by far the best magnetocaloric material near room temperature. Due to its large density of 9.95 g cm^{-3}, it can pump significantly more heat than La–Fe–Si–Mn–H. It is also apparent that Fe–Rh can provide a high level effect over a wide temperature range, whereas for all the other materials shown in Figure 7 the reversible heat drops down rapidly on the left- and right-hand sides of the maximum. This is related to the shift of the transition temperature and the sharpness of the transformation, which are both outstanding for Fe–Rh.

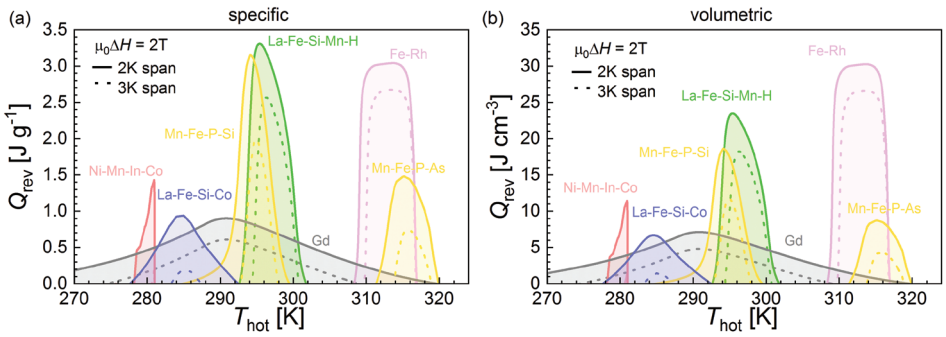

Figure 7. Comparison of different magnetocaloric materials in terms of their reversible heat that can be extracted in one thermodynamic Carnot cycle with a temperature span of 2 K (solid lines) and 3 K (dotted lines). The specific Q_{rev} is plotted in (a) and the volumetric counterpart is shown in (b).

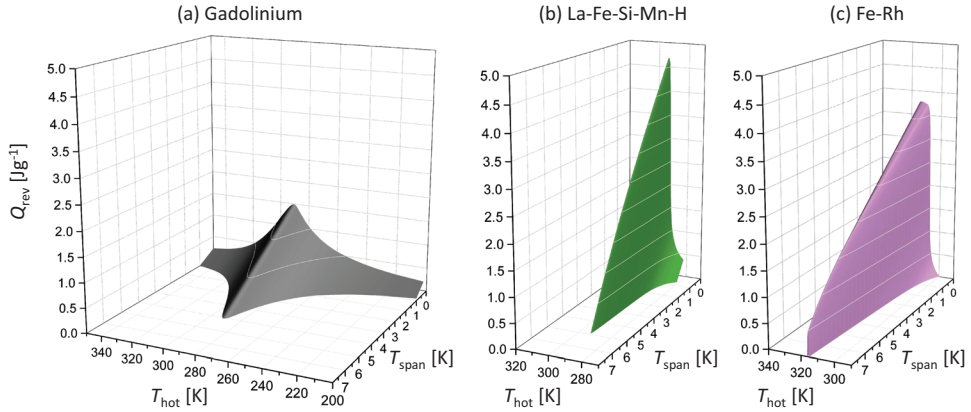

Figure 8. 3D representation of the reversible heat as a function of hot heat exchanger temperature and the temperature span of a) gadolinium, b) La–Fe–Si–Mn–H, and c) Fe–Rh for a magnetic field change of 2 T.

We could get the impression that gadolinium performs poorly in comparison to the other compounds. This is true in terms of the amount of heat that can be transferred, due to the relatively low isothermal entropy change Δs_T. But in fact the situation is more complex, since a cooling device that cannot provide a certain temperature difference between the cooling compartment and the surroundings is useless. Pure gadolinium can operate over a very broad temperature range, with a moderate Q_{rev} and the same holds true for La–Fe–Si–Co. Even though the latter has a much smaller ΔT_{ad}, because of the shape of the $s(T)$ diagram, La–Fe–Si–Co can pump similar amounts of heat to Gd. Furthermore, it is evident from Figure 7 that a single batch of La–Fe–Si–Mn–H cannot compete, since its working range is simply too small. In fact, four or five layers would be required to create a similar temperature difference between the hot and the cold end of the material compartment. The manufacturing and operating of such a stacked heat exchanger is not that simple, for obvious reasons, but it definitely has the potential to outperform gadolinium.

Several important issues need to be addressed concerning the figure of merit. Here, we focused on Carnot cycles with temperature spans of 2 and 3 K in 2 T. This limit is already set fairly high. We can draw a different diagram, for instance, for the pair of 2 K and 1 T that is even harder. Only a few known magnetocaloric materials can provide such a large cyclic ΔT_{ad} in order to work under these conditions. This example shows how challenging it is to describe magnetocaloric materials by a single value. Strictly speaking, the reversible heat, temperature, entropy change, etc. are multidimensional objects. **Figure 8** illustrates Q_{rev} as a function of the hot heat exchanger temperature and the span for gadolinium, La–Fe–Si–Mn–H and Fe–Rh for a magnetic field change of 2 T leading to spark-like structures. Consequently, a reasonable materials description can only succeed when specifying realistic operational conditions.

6. Summary

In this article we were discussing the relevant properties of the most promising magnetocaloric materials for solid-state refrigeration. In particular, we provide a comprehensive analysis of the cyclability of those systems, but also magnetic, calorimetric, heat transfer, and criticality aspects need to be considered for a thorough comparison. When dealing with first-order types of transitions, special care must be taken in order to monitor the reversibility in the correct manner. The reversible adiabatic temperature change ΔT_{ad} and the isothermal entropy changes Δs_T in magnetic-field changes of 1 and 2 T around the transition temperature T_t play the key role since they define the operating window and the amount of heat that can be transferred. The magnetization change ΔM, the hysteresis width ΔT_{hys} and the shift of the transition temperature in magnetic fields $\frac{dT_t}{dH}$ are other factors for first-order transition materials. Together with the heat capacity c_p, they determine the size of the reversible magnetocaloric effect. Those specifications (if applicable) are given for the different materials in the Table 1 as well as the application-related properties of thermal conductivity λ and the density ρ. The latter two are often disregarded. Concerning the reversible adiabatic temperature change, $La_{0.7}Ca_{0.3}MnO_3$ and $Ni_{45.7}Mn_{36.6}In_{13.5}Co_{4.2}$ show almost similar effects in a field change of 2 T. Since the manganites are oxidic compounds, their thermal conductivity is very poor (λ = 1.5 W m^{-1} K^{-1}) whereas Heusler alloys turn out to be among the most thermal conductive magnetocaloric materials (λ = 23.5 W m^{-1} K^{-1}). A magnetocaloric heat exchanger can only be efficient when it is capable of absorbing or releasing heat from or to the exchange fluid. This issue actually goes far beyond the thermal conductivity alone, since it essentially depends on the design of the heat exchanger, the surface characteristics, the properties of the fluid and its flow type, to mention just some. As a figure of merit we utilize the transferable heat Q_{rev} of a Carnot cycle for given temperature spans and magnetic-field changes. With the density ρ it is also possible to plot the volumetric Q_{rev}. This parameter allows us to compare both the working range and the magnetocaloric strength of different materials. Based on our experimental study, the following conclusions can be drawn for the room-temperature range:

- in a field change of 1 T, so far no magnetocaloric material operating near room temperature has a larger reversible ΔT_{ad} than gadolinium;
- La–Fe–Si–Co can provide similar Q_{rev} values to gadolinium

for a 2 K temperature span and a 2 T field change across a rather broad operating window;

- Fe–Rh is the best material in terms of the amount of heat that can be pumped reversibly per unit volume, but at the same time it is among the most critical materials;
- La–Fe–Si–Mn–H and Mn–Fe–P–Si are the most promising noncritical alternatives for room-temperature application and can outperform Gd in terms of Q_{rev}.

7. Conclusion

Under the prerequisite that high-quality stacks of first-order materials with different T_ts can be produced, we can conclude that the larger the magnetic field change of the refrigerator, the better the performance of these alternatives to gadolinium becomes and the easier it will be to build an energy-efficient and noncritical heat exchanger. However, this leads to an impasse since from a technical and economic point of view, a conventional AMR machine with a magnetic field source made of permanent magnets is limited to a field change of about 1 T.[73] The use of electromagnets and superconducting solenoids can in principle generate larger fields, but we face different issues.[8] In any case, a further improvement of known compounds and their hysteresis reduction are indispensable unless we find new, noncritical magnetocaloric materials that can outperform gadolinium. The evolving field of computational material science could open this door.

An alternative route for solid-state refrigeration is multicaloric cooling.[74] This approach relies on multiferroic materials that have a susceptibility to more than one external field.[75] There are two possibilities to realize such a cooling cycle, either by using a single multicaloric material[76] or a composite.[77] The direct combination of two stimuli could help to increase the caloric response due to the potentially higher field strength. However, the coupling mechanisms in multicaloric materials are complex and require further investigation.[74] There is also the possibility of a multicaloric cycle in which the thermal hysteresis of first-order materials can be exploited.[78] Using this approach, the quantity of permanent magnets needed can be reduced drastically and at the same time the field strength can be increased. The development of the first multicaloric demonstrators is still pending. More progress in this field requires that the different communities of magneto-, electro- and elastocaloric cooling work hand in hand with system engineers.

8. Outlook

We live in a cryogenic age![79] Refrigerators and air conditioning systems have become so commonplace that people are hardly aware about their existence and consequences. Today, our conventional cooling technology causes already about 8% of global CO_2 emissions, tendency strongly increasing, more than the global aviation, and shipping industry together. The great environmental impact and the growing hunger of mankind for artificial cold in the course of this century makes it inevitable to rethink how we are going to deal with our natural resources and the climate on this planet. A sustainable change can only be achieved on different levels simultaneously. Scientist and engineers have to come up with new refrigeration technologies that are environmentally friendly throughout the entire product life cycle, replacing the existing one which is essentially unchanged for more than 100 years, but also trade and industry must contribute to the reorganization of our social economics. Last but not least, every individual has to reconsider the use of refrigeration so that all people in the world gain equal access to cooling one day.

Supporting Information

Supporting Information is available from the Wiley Online Library or from the author.

Acknowledgements

This work was supported by the European Research Council (ERC) under the European Unions Horizon 2020 research and innovation programme (Grant No. 743116-project Cool Innov), by the DFG (Grant No. SPP 1599), by the Helmholtz Association via the Helmholtz-RSF Joint Research Group (Project No. HRSF-0045), by the HLD at HZDR, a member of the European Magnetic Field Laboratory (EMFL), by DFG in the framework of the Excellence Initiative, Darmstadt Graduate School of Excellence Energy Science and Engineering (Grant No. GSC 1070) and by the European Community 7th Framework Program (Grant No. 310748 DRREAM). Special thanks goes to many people who contribute with samples and/or data: M. Acet, E. Brück, R. Burriel, A. Chirkova, L. Cohen, F. Guillou, V. Pecharsky, and J. Turcaud. The equation on page one relating to ΔT_{ad} was corrected on September 12, 2019.

Conflict of Interest

The authors declare no conflict of interest.

Keywords

magnetic cooling, magnetocaloric effect, solid-state refrigeration

Received: April 23, 2019
Revised: July 1, 2019
Published online: July 31, 2019

[1] O. Gutfleisch, M. A. Willard, E. Brück, C. H. Chen, S. G. Sankar, J. P. Liu, *Adv. Mater.* **2011**, *23*, 821.
[2] S. Fähler, U. K. Rößler, O. Kastner, J. Eckert, G. Eggeler, H. Emmerich, P. Entel, S. Müller, E. Quandt, K. Albe, *Adv. Eng. Mater.* **2012**, *14*, 10.
[3] J. Liu, T. Gottschall, K. P. Skokov, J. D. Moore, O. Gutfleisch, *Nat. Mater.* **2012**, *11*, 620.
[4] X. Moya, L. E. Hueso, F. Maccherozzi, A. I. Tovstolytkin, D. I. Podyalovskii, C. Ducati, L. C. Phillips, M. Ghidini, O. Hovorka, A. Berger, M. E. Vickers, E. Defay, S. S. Dhesi, N. D. Mathur, *Nat. Mater.* **2013**, *12*, 52.
[5] I. Takeuchi, K. Sandeman, *Phys. Today* **2015**, *68*, 48.
[6] M. Balli, O. Sari, C. Mahmed, C. Besson, P. Bonhote, D. Duc, J. Forchelet, *Appl. Energy* **2012**, *98*, 556.

[7] K. Engelbrecht, D. Eriksen, C. Bahl, R. Bjørk, J. Geyti, J. Lozano, K. Nielsen, F. Saxild, A. Smith, N. Pryds, *Int. J. Refrig.* **2012**, *35*, 1498.
[8] A. Kitanovski, U. Plaznik, U. Tomc, A. Poredoš, *Int. J. Refrig.* **2015**, *57*, 288.
[9] B. Yu, M. Liu, P. W. Egolf, A. Kitanovski, *Int. J. Refrig.* **2010**, *33*, 1029.
[10] F. Scarpa, G. Tagliafico, L. A. Tagliafico, *Renewable Sustainable Energy Rev.* **2015**, *50*, 497.
[11] J. M. Belman-Flores, J. M. Barroso-Maldonado, A. P. Rodríguez-Muñoz, G. Camacho-Vázquez, *Renewable Sustainable Energy Rev.* **2015**, *51*, 955.
[12] J. R. Gómez, R. F. Garcia, A. D. M. Catoira, M. R. Gómez, *Renewable Sustianable Energy Rev.* **2013**, *17*, 74.
[13] K. P. Skokov, A. Y. Karpenkov, D. Y. Karpenkov, O. Gutfleisch, *J. Appl. Phys.* **2013**, *113*, 17A945.
[14] R. Bjørk, C. Bahl, K. Nielsen, *Int. J. Refrig.* **2016**, *63*, 48.
[15] M. Fries, L. Pfeuffer, E. Bruder, T. Gottschall, S. Ener, L. V. Diop, T. Gröb, K. P. Skokov, O. Gutfleisch, *Acta Mater.* **2017**, *132*, 222.
[16] T. Gottschall, K. P. Skokov, F. Scheibel, M. Acet, M. G. Zavareh, Y. Skourski, J. Wosnitza, M. Farle, O. Gutfleisch, *Phys. Rev. Appl.* **2016**, *5*, 024013.
[17] M. G. Zavareh, Y. Skourski, K. P. Skokov, D. Y. Karpenkov, L. Zvyagina, A. Waske, D. Haskel, M. Zhernenkov, J. Wosnitza, O. Gutfleisch, *Phys. Rev. Appl.* **2017**, *8*, 014037.
[18] A. Smith, C. R. Bahl, R. Bjørk, K. Engelbrecht, K. K. Nielsen, N. Pryds, *Adv. Eng. Mater.* **2012**, *2*, 1288.
[19] F. Qin, N. Bingham, H. Wang, H. Peng, J. Sun, V. Franco, S. Yu, H. Srikanth, M. Phan, *Acta Mater.* **2013**, *61*, 1284.
[20] D. Vuarnoz, T. Kawanami, *Appl. Therm. Eng.* **2012**, *37*, 388.
[21] K. P. Skokov, D. Y. Karpenkov, M. D. Kuz'min, I. A. Radulov, T. Gottschall, B. Kaeswurm, M. Fries, O. Gutfleisch, *J. Appl. Phys.* **2014**, *115*, 17A941.
[22] I. A. Radulov, K. P. Skokov, D. Y. Karpenkov, T. Gottschall, O. Gutfleisch, *J. Mag. Mag. Mater.* **2015**, *396*, 228.
[23] D. Ramirez, L. Murr, S. Li, Y. Tian, E. Martinez, J. Martinez, B. Machado, S. Gaytan, F. Medina, R. Wicker, *Mater. Sci. Eng. A* **2011**, *528*, 5379.
[24] J. D. Moore, D. Klemm, D. Lindackers, S. Grasemann, R. Träger, J. Eckert, L. Löber, S. Scudino, M. Katter, A. Barcza, K. P. Skokov, O. Gutfleisch, *J. Appl. Phys.* **2013**, *114*, 043907.
[25] J. Lyubina, R. Schäfer, N. Martin, L. Schultz, O. Gutfleisch, *Adv. Mater.* **2010**, *22*, 3735.
[26] V. Franco, J. Blázquez, B. Ingale, A. Conde, *Annu. Rev. Mater. Sci.* **2012**, *42*, 305.
[27] A. Giguère, M. Foldeaki, B. R. Gopal, R. Chahine, T. K. Bose, A. Frydman, J. A. Barclay, *Phys. Rev. Lett.* **1999**, *83*, 2262.
[28] O. Cakir, M. Acet, *Appl. Phys. Lett.* **2012**, *100*, 202404.
[29] M. D. Kuz'min, *Appl. Phys. Lett.* **2007**, *90*, 251916.
[30] A. Kitanovski, P. W. Egolf, *Int. J. Refrig.* **2010**, *33*, 449.
[31] A. Waske, L. Giebeler, B. Weise, A. Funk, M. Hinterstein, M. Herklotz, K. Skokov, S. Fähler, O. Gutfleisch, J. Eckert, *Phys. Status Solidi RRL* **2015**, *9*, 136.
[32] T. Gottschall, D. Benke, M. Fries, A. Taubel, I. A. Radulov, K. P. Skokov, O. Gutfleisch, *Adv. Funct. Mater.* **2017**, *27*, 1606735.
[33] V. V. Khovaylo, K. P. Skokov, O. Gutfleisch, H. Miki, R. Kainuma, T. Kanomata, *Appl. Phys. Lett.97*, **2010**, 052503.
[34] A. Fujita, Y. Akamatsu, K. Fukamichi, *J. Appl. Phys.* **1999**, *85*, 4756.
[35] S. Y. Dan'kov, A. M. Tishin, V. K. Pecharsky, K. A. Gschneidner, *Phys. Rev. B* **1998**, *57*, 3478.
[36] J. Y. Law, V. Franco, L. M. Moreno-Ramrez, A. Conde, D. Y. Karpenkov, I. Radulov, K. P. Skokov, O. Gutfleisch, *Nat. Commun.* **2018**, *9*, 2680.
[37] T. Gottschall, M. D. Kuz'min, K. P. Skokov, Y. Skourski, M. Fries, O. Gutfleisch, M. G. Zavareh, D. L. Schlagel, Y. Mudryk, V. Pecharsky, J. Wosnitza, *Phys. Rev. B* **2019**, *99*, 134429.
[38] T. Krenke, E. Duman, M. Acet, E. F. Wassermann, X. Moya, L. Mañosa, A. Planes, *Nat. Mater.* **2005**, *4*, 450.
[39] E. Stern-Taulats, A. Gràcia-Condal, A. Planes, P. Lloveras, M. Barrio, J.-L. Tamarit, S. Pramanick, S. Majumdar, L. Mañosa, *Appl. Phys. Lett.* **2015**, *107*.
[40] A. Chirkova, K. Skokov, L. Schultz, N. Baranov, O. Gutfleisch, T. Woodcock, *Acta Mater.* **2016**, *106*, 15.
[41] L. Morellon, J. Blasco, P. Algarabel, M. Ibarra, *Phys. Rev. B: Condens. Matter Mater. Phys.* **2000**, *62*, 1022.
[42] N. H. Dung, L. Zhang, Z. Q. Ou, E. Brück, *Scr. Mater.* **2012**, *67*, 975.
[43] E. Stern-Taulats, P. O. Castillo-Villa, L. Mañosa, C. Frontera, S. Pramanick, S. Majumdar, A. Planes, *J. Appl. Phys.* **2014**, *115*, 173907.
[44] L. Mañosa, D. González-Alonso, A. Planes, M. Barrio, J.-L. Tamarit, I. S. Titov, M. Acet, A. Bhattacharyya, S. Majumdar, *Nat. Commun.* **2011**, *2*, 595.
[45] O. Tegus, E. Brück, K. H. J. Buschow, F. R. de Boer, *Nature* **2002**, *415*, 150.
[46] O. Gutfleisch, T. Gottschall, M. Fries, D. Benke, I. Radulov, K. P. Skokov, H. Wende, M. Gruner, M. Acet, P. Entel, M. Farle, *Philos. Trans. R. Soc., A* **2016**, *374*, 20150308.
[47] K. Navickaitė, H. N. Bez, T. Lei, A. Barcza, H. Vieyra, C. R. Bahl, K. Engelbrecht, *Int. J. Refrig.* **2018**, *86*, 322.
[48] T. Gottschall, K. P. Skokov, R. Burriel, O. Gutfleisch, *Acta Mater.* **2016**, *107*, 1.
[49] B. Kaeswurm, V. Franco, K. P. Skokov, O. Gutfleisch, *J. Mag. Mag. Mater.* **2016**, *406*, 259.
[50] J. Liu, J. Moore, K. Skokov, M. Krautz, K. Löwe, A. Barcza, M. Katter, O. Gutfleisch, *Scr. Mater.* **2012**, *67*, 584.
[51] A. Kitanovski, J. Tušek, U. Tomc, U. Plaznik, M. Ožbolt, A. Poredoš, *Magnetocaloric Energy Conversion: From Theory to Applications*. Green Energy and Technology, Springer International Publishing, Switzerland **2014**.
[52] R. Moss, E. Tzimas, P. Willis, J. Arendorf, P. Thompson, A. Chapman, N. Morley, E. Sims, R. Bryson, J. Pearson, L. Tercero Espinoza, Technical report, European Union, **2013**.
[53] S. Glöser, L. T. Espinoza, C. Gandenberger, M. Faulstich, *Resource Policy* **2015**, *44*, 35.
[54] European Commission, COM(2017) 490, 2017.
[55] European Commission, Report on Critical Raw Materials for the EU—Report of the Ad hoc Working Group on defining critical raw materials, 2014.
[56] R. Gauß, O. Gutfleisch, *Magnetische Materialien — Schlüsselkomponenten für neue Energietechnologien*, Springer, Berlin/Heidelberg **2016**, pp. 99–118.
[57] R. Gauß, G. Homm, O. Gutfleisch, *J. Ind. Ecol.* **2016**, *21*, 1291.
[58] V. K. Sharma, M. K. Chattopadhyay, S. B. Roy, *J. Phys. D: Appl. Phys.* **2007**, *40*, 1869.
[59] M.-H. Phan, S.-C. Yu, *J. Magn. Magn. Mater.* **2007**, *308*, 325.
[60] F. Guillou, H. Yibole, G. Porcari, L. Zhang, N. H. van Dijk, E. Brück, *J. Appl. Phys.* **2014**, *116*, 063903.
[61] K. Engelbrecht, C. R. H. Bahl, *J. Appl. Phys.* **2010**, *108*, 123918.
[62] S. Qian, D. Nasuta, A. Rhoads, Y. Wang, Y. Geng, Y. Hwang, R. Radermacher, I. Takeuchi, *Int. J. Refrig.* **2016**, *62*, 177.
[63] L. D. Griffith, Y. Mudryk, J. Slaughter, V. K. Pecharsky, *J. Appl. Phys.* **2018**, *123*, 034902.
[64] J. Turcaud, Ph.D. thesis, Imperial College London, **2014**.
[65] V. K. Pecharsky, K. A. Gschneidner Jr., *Phys. Rev. Lett.* **1997**, *78*, 4494.
[66] K. P. Skokov, K.-H. Müller, J. D. Moore, J. Liu, A. Y. Karpenkov, M. Krautz, O. Gutfleisch, *J. Alloys Compd.* **2013**, *552*, 310.
[67] K. Morrison, K. Sandeman, L. Cohen, C. Sasso, V. Basso, A. Barcza, M. Katter, J. Moore, K. Skokov, O. Gutfleisch, *Int. J. Ref.* **2012**, *35*, 1528.

[68] F. Guillou, G. Porcari, H. Yibole, N. van Dijk, E. Brück, *Adv. Mater.* **2014**, *26*, 2671.
[69] T. Gottschall, K. P. Skokov, B. Frincu, O. Gutfleisch, *Appl. Phys. Lett.* **2015**, *106*, 021901.
[70] F. Scheibel, T. Gottschall, K. Skokov, O. Gutfleisch, M. Ghorbani-Zavareh, Y. Skourski, J. Wosnitza, Ö. Cakir, M. Farle, M. Acet, *J. Appl. Phys.* **2015**, *117*, 233902.
[71] M. Annaorazov, H. Güven, K. Bärner, *J. Alloys Compd.* **2005**, *397*, 26.
[72] T. Gottschall, E. Stern-Taulats, L. Mañosa, A. Planes, K. P. Skokov, O. Gutfleisch, *Appl. Phys. Lett.* **2017**, *110*, 223904.
[73] R. Bjørk, A. Smith, C. Bahl, N. Pryds, *Int. J. Refrig.* **2011**, *34*, 1805.
[74] A. Planes, T. Castán, A. Saxena, *Philos. Trans. R. Soc. A* **2016**, *374*.
[75] A. S. Starkov, O. V. Pakhomov, V. V. Rodionov, A. A. Amirov, I. A. Starkov, *Tech. Phys. Lett.* **2018**, *44*, 243.
[76] X. Moya, S. Kar-Narayan, N. D. Mathur, *Nat. Mater.* **2014**, *13*, 439.
[77] Y. Liu, L. C. Phillips, R. Mattana, M. Bibes, A. Barthélémy, B. Dkhil, *Nat. Commun.* **2016**, *7*, 11614.
[78] T. Gottschall, A. Grácia-Condal, M. Fries, A. Taubel, L. Pfeuffer, L. Mañosa, A. Planes, K. P. Skokov, O. Gutfleisch, *Nat. Mater.* **2018**, *17*, 929.
[79] A. Friedrich, presented at *Thermag VIII*. Int. Conf. on Caloric Cooling, TU Darmstadt, September **2018**.